



Published in final edited form as:

*Metabolomics*. 2012 ; 8(6): 989–996. doi:10.1007/s11306-011-0395-z.

## A Carbonyl Capture Approach for Profiling Oxidized Metabolites in Cell Extracts

Stephanie J. Mattingly<sup>‡</sup>, Tao Xu<sup>‡</sup>, Michael H. Nantz<sup>\*</sup>, Richard M. Higashi, and Teresa W.-M. Fan<sup>\*</sup>

Department of Chemistry and Center for Regulatory and Environmental Analytical Metabolomics (CREAM), University of Louisville, Louisville, KY, 40292, USA

### Abstract

Fourier-transform ion-cyclotron resonance mass spectrometry (FT-ICR-MS) detection of oxidized cellular metabolites is described using isotopologic, carbonyl-selective derivatizing agents that integrate aminoxy functionality for carbonyl capture, quaternary nitrogen for electrospray enhancement, and a hydrophobic domain for sample cleanup. These modular structural features enable rapid, sensitive analysis of complex mixtures of metabolite-derivatives by FT-ICR-MS via continuous nanoelectrospray infusion. Specifically, this approach can be used to globally assess levels of low abundance and labile aldehyde and ketone metabolites quantitatively and in high throughput manner. These metabolites are often key and unique indicators of various biochemical pathways and their perturbations. Analysis of lung adenocarcinoma A549 cells established a profile of carbonyl metabolites spanning multiple structural classes. We also demonstrate a procedure for metabolite quantification using pyruvate as a model analyte.

### Keywords

metabolite profiling; mass spectrometry; ketone; aldehyde; cellular oxidation state; pyruvate;  $\alpha$ -ketoglutarate; oxaloacetate

## 1 Introduction

The analysis of cellular aldehyde and ketone species is of considerable importance in the field of metabolomics since carbonyl species are pervasive intermediates of normal metabolism as well as common products of oxidative stress (Zajdel *et al.*, 2007); (Noda *et al.*, 2007), which has been implicated in the pathogenesis of many diseases including cancer (Negre-Salvayre *et al.*, 2010). Indeed, the detection and identification of oxidized cellular species, in general, has become an important focus of research efforts in metabolomics where potential early markers of disease are sought (Griffiths *et al.*, 2010; Psychogios *et al.*, 2011); Griffiths *et al.* 2010; (Wikoff *et al.*, 2009). The identification of polar aldehyde and ketone metabolites from aqueous cell extracts is particularly challenging owing to their low-abundance, high reactivity, and the difficulties associated with their extraction from the cell matrix. Mass spectrometry has the sensitivity required for observing these low-abundant species, but due to insufficient mass accuracy and resolution, most MS methods are coupled with chromatography to distinguish analytes with similar  $m/z$ .

<sup>\*</sup>Corresponding authors: teresa.fan@louisville.edu, michael.nantz@louisville.edu, phone: (502) 852-6448, (502) 852-8069, fax: (502) 852-7214, (502) 852-7214.

<sup>‡</sup>These authors contributed equally to this work

Fourier-transform ion-cyclotron resonance MS (FT-ICR-MS), however, does not suffer these limitations for low-molecular mass analytes and can provide unique molecular formulae of most metabolites. In addition, FT-ICR-MS can achieve simultaneous resolution of  $^{13}\text{C}$  isotopologues and distinguish them from other elemental (such as  $^{15}\text{N}$  or D) isotopologues (Lane *et al.*, 2009); (Lane *et al.*, 2008). However, direct infusion FT-ICR-MS is often compromised by unstable sample introduction (e.g., electrospray) and low ion yields due to interference from cellular salts and/or interaction with matrix ions in aqueous biological extracts. Consequently, metabolite derivatization is a strategy that can be employed to overcome these challenges.

In the case of aldehyde and ketone metabolites, derivatization is commonly performed to facilitate liquid chromatography with optical or MS detection (LC-MS) or gas chromatography coupled to mass spectrometry (GC-MS). Such derivatization reagents either have distinct absorbances (for optical detection), preserve or increase volatility (GC), or have easily ionizable groups for MS detection, such as those exemplified in Figure 1 (Eggink *et al.*, 2010; Iglesias *et al.*, 2010; Maboudou *et al.*, 2002); (Zajdel *et al.*, 2007); (Sugaya *et al.*, 2004); (Barry *et al.*, 2003); Maboudou *et al.* 2002; (Wheeler, 1968)). These reagents react with carbonyls via their amine (Eggink *et al.*, 2010), hydrazine (Maboudou *et al.*, 2002), hydrazide (Griffiths *et al.*, 2008) (Hong and Wang, 2007) (Johnson, 2007) or aminoxy (Iglesias *et al.*, 2010) (Sugaya *et al.*, 2004) moieties to form corresponding imine, hydrazone, acyl hydrazone, or oxime ether adducts, respectively. Some of these reagents also employ a permanent positive charge to enhance electrospray MS sensitivity (Eggink *et al.*, 2010) (Griffiths *et al.*, 2008) (Hong and Wang, 2007) (Johnson, 2007) (Barry *et al.*, 2003) (Mark M. Ross, 1985) (Wheeler, 1968). The disadvantages in the reported approaches include multistep procedures for metabolite derivatization and/or lengthy chromatographic separation of the resultant metabolite adducts.

Our aim to use direct infusion FT-ICR-MS to analyze crude biological extracts led us to the development of a permanently charged reagent for ready conversion of carbonyl metabolites into stable, non-volatile, charged adducts. Thus, our reagent design included compatibility with aqueous medium, suitable hydrophobicity for partitioning the charged adducts into an organic solvent for optimal electrospray stability, and formation of adducts with sufficient molecular mass to exploit the sensitive  $m/z$  range of the FT-ICR-MS, which is higher than  $m/z$  150 based on our experience. We report here a new, permanently cationic amphiphile that meets these functional criteria and demonstrate its application in the global profiling of oxo-metabolites directly from crude aqueous extracts of cancer cells.

## 2. Materials and Methods

### 2.1 Synthesis of derivatizing agents QDA and \*QDA

*N*-[2-(Aminoxy)ethyl]-*N,N*-dimethyl-1-dodecylammonium iodide (QDA) and \*QDA ( $^{13}\text{C}_3$ -labeled QDA) were prepared as outlined in Scheme S1 (Supplementary information) according to our previously published method (Biswas *et al.*, 2010) for the synthesis of structurally related aminoxy compounds using the Mitsunobu approach originally described by Grochowski and Jurczak (1976). Full experimental and characterization details are provided in the Supplementary Information.

### 2.2 Cell culturing and extraction of polar metabolites

Human lung adenocarcinoma A549 cells were grown in 10-cm plates with 8 mL RPMI 1640 medium (Sigma) supplemented with 2 mM glutamine, 0.2% glucose, 10% fetal bovine serum, 100 U/mL penicillin, and 0.1 mg/mL streptomycin at 37°C, 5% CO<sub>2</sub> and 95% humidity. When cells became 70% confluent, the medium was removed, and the cells were

washed quickly three times on ice each with 5 ml cold 1X PBS (phosphate buffered saline) to remove medium components. After PBS was drained via vacuum suction, 1 ml of cold acetonitrile (-20 °C) was added immediately to quench metabolism within seconds by precipitating proteins. Then, 0.75 mL of nanopure water was added before cells were scraped and collected into a 15 mL polypropylene conical centrifuge tube (Sarstedt, Newton, NC) containing three 3 mm diameter glass beads. These steps were then repeated to collect any remaining cells. Next, 1 mL HPLC-grade chloroform (Fisher Scientific) was added to the centrifuge tube containing the cell lysate and the mixture was shaken vigorously. Partitioning of polar and non-polar metabolites into aqueous and solvent layers was performed as described previously (Fan *et al.*, 2011; Lorkiewicz *et al.*, 2011). The aqueous extract was lyophilized and stored at -80 °C prior to analysis.

### 2.3 Metabolite Derivatization and adduct extraction

50 µL of a 1:1 mixture of 100 µM QDA and \*QDA dissolved in nanopure water was added to a 1.5 mL microcentrifuge tube containing the aqueous extract of approximately one quarter of a 10 cm cell plate in 50 µL of 10 mM pH 6 NH<sub>4</sub>OAc buffer. The tube was briefly vortexed, sonicated for 1 hr and placed in a 40 °C dry bath for 23 hours. This reaction time was chosen because increased ion counts were observed up to 23h of reaction time in 63% of the metabolites assigned, even though 85% of all assigned metabolites were observable after 30 minute of reaction time. Following reaction, the aqueous layer was extracted with *n*-butanol three times, and dried by vacuum centrifugation (Vacufuge, Eppendorf, Hauppauge, NY). The residue was dissolved in methanol with 0.1% v/v formic acid and analyzed by FT-ICR-MS as a 1:1 mixture with an external standard of 2 µM (*N,N*-dimethyl-*N*-(2-((D<sub>6</sub>-propan-2-ylideneamino)oxy)ethyl)octan-1-aminium iodide) in methanol. For each experiment, three replicate samples were analyzed. A buffer blank consisting of 50 µL 10 mM pH 6 NH<sub>4</sub>OAc buffer and 50 µL of the QDA/\*QDA mixture was prepared and analyzed similarly to serve as a negative control.

### 2.4 FT-ICR-MS analysis

Samples were analyzed on a hybrid linear ion trap (LIT) FT-ICR mass spectrometer (LTQ-FT, Thermo Electron, Bremen, Germany) equipped with a TriVersa NanoMate ion source (Advion BioSciences, Ithaca, NY) with an “A” electrospray chip (nozzle inner diameter 5.5 µm). The TriVersa NanoMate was operated in positive ion mode by applying 1.85 kV with 0.1 psi head pressure. MS runs were recorded over a mass range from 150 to 1200 Da. Initially, low resolution LIT-MS scans were acquired for 0.75 minute to track the stability of the ion spray, after which high mass accuracy data were collected using the FT-ICR analyzer where MS scans were acquired for 8 min and at the target mass resolution of 1 in 400,000 *m/z*. The AGC (automatic gain control) maximum ion time was set to 10 ms and 500 ms for the LIT and ICR operations, respectively, using default ion count targets for both. Five “microscans” (ICR transients) were accumulated before Fourier transformation to produce each saved spectrum; thus the cycle time for each transformed, saved spectrum was about 5 s. The LTQ-FT was tuned and calibrated according to the manufacturer’s default standard recommendations, which typically achieved better than 0.2 ppm mass accuracy at 400,000 resolving power at *m/z* = 400.

FT-ICR mass spectra were exported as exact mass lists into an Excel file using QualBrowser 2.0 SR2 (Thermo Electron, “Bremen” version for the LTQ-FT). QDA/\*QDA adducts were assigned based on their accurate mass by using an in-house software tool PREMISE (PREcalculated Exact Mass Isotopologue Search Engine)(Lane *et al.*, 2009) and by manual validation. PREMISE is a simple algorithm that corrects small measured mass errors based on a known peak (such as internal standard, or a known analyte), then matches the corrected observed *m/z* with theoretical *m/z* values using a selectable *m/z* window typically set to

0.0008 Da or smaller. The theoretical  $m/z$  values of a large number of QDA-metabolite adducts were calculated and compiled in a reference table for the PREMISE assignment.

## 2.5 Global assignment of carbonyl metabolites based on their QDA-adducts and companion \*QDA-adducts

QDA and \*QDA adduct mixtures from 2.3 were acquired for nine minutes on FT-ICR-MS as described in 2.4 and spectra were averaged over all saved scans. Next, all peaks from each acquisition were exported as exact mass lists to Excel. Any peaks with ion counts less than 1000 were deleted to eliminate noise. A theoretical “+4”  $m/z$  list was created by adding 4.02188 ( $1 \times {}^{13}\text{C} + 3 \times \text{D}$  mass) to all remaining peaks in the list. PREMISE software was then used to find matches between the experimental peak list and the calculated +4 peak list with an error window of 0.0009  $m/z$ . This simplified list was then crosschecked manually against the negative control peak list and any duplicate masses were deleted, except in cases where the intensity was significantly higher in the sample than the negative control (>80%). Where multiple +4 peaks (\*QDA adducts) were matched, the peaks with ion counts most closely matching that of the QDA adduct peak were retained. The final exact mass list was used to deduce the corresponding molecular formulae of the adducts and thereby the parent carbonyl metabolites. The metabolites, in turn, were assigned by matching the formulae against those in our custom database comprised of a large number of known carbonyl metabolites.

## 2.6 Quantification of pyruvate in cell extracts

For accurate quantification of carbonyl metabolites by the QDA method, several factors need to be considered: (a) concentration range with linear instrumental response; (b) ion suppression effects of extract matrix; (c) pKa shifts of ionizable groups due to the presence of other ions in cell-extracts; (d) partition efficiency; and (e) reaction efficiency (a consequence of the equilibria of carbonyl species with unreactive forms, such as hydrates, enols (Fang *et al.*, 2010), and imines). Each of these factors can affect ion counts and thus compromise accurate quantification of a given carbonyl metabolite. Nonetheless, an estimate of the impact of these factors on quantification can be made.

We selected pyruvate as a representative metabolite and verified its linear instrumental response from 0.025–25  $\mu\text{M}$  (see Figure S1 in Supplementary Information). Next, we established an internal standard curve for cell extract samples by adding variable amounts of  ${}^{13}\text{C}_3$ -labeled pyruvate (see below) to cell extracts before derivatizing them with QDA; this allowed us to correct for the partition and reaction efficiency. Finally, ion suppression in the cell extracts was accounted for by normalizing against independently-reacted, non-extracted, \*QDA-pyruvate added at the same concentration to all FT-MS samples as an external standard. Thus, three mass isotopologues of the pyruvate adduct were made for quantification purpose: QDA-pyruvate (from pyruvate extant in the cellular extract), a reaction standard (QDA- ${}^{13}\text{C}_3$ -pyruvate), and an external standard (\*QDA-pyruvate).

Five, 10 or 15  $\mu\text{L}$  of 100  $\mu\text{M}$  uniformly  ${}^{13}\text{C}$  labeled sodium pyruvate ( ${}^{13}\text{C}_3$ -pyruvate) in 10 mM  $\text{NH}_4\text{OAc}$  buffer was added to three 1.5 mL microcentrifuge tubes containing the aqueous extract of approximately one quarter of a 10 cm cell plate in 10 mM  $\text{NH}_4\text{OAc}$  buffer such that the total volume of buffer was kept at 50  $\mu\text{L}$ . 50  $\mu\text{L}$  of 200  $\mu\text{M}$  QDA in nanopure water was then added. The tube was briefly vortexed, sonicated for 1 hr and placed in a 40 °C dry bath for 23 hours. Following reaction, the aqueous layer was extracted with *n*-butanol three times, and dried (as above). The residue was dissolved in methanol with 0.1% (v/v) formic acid. Negative controls were prepared by replacing cell extract with buffer.

For preparation of the external standard, 110  $\mu\text{L}$  of 1 mM \*QDA in nanopure water was added to 100  $\mu\text{L}$  of 1 mM unlabeled sodium pyruvate in buffer. This solution was likewise

vortexed, sonicated, and heated for 24 hours, after which, the aqueous solution (without extraction) was dried on a vacufuge. The extracts containing  $^{13}\text{C}$  labeled pyruvate were diluted 1:1 with the external standard solution (final \*QDA-pyruvate concentration of 2.5  $\mu\text{M}$  in methanol with 0.1 % formic acid) and then analyzed by FT-ICR-MS. Each analysis was repeated three times.

For an estimate of the “ion suppression” (loss of signal intensity) factor in cellular extracts, the ion counts of QDA-pyruvate and QDA- $^{13}\text{C}_3$ -pyruvate peaks were obtained and normalized against that of the external standard \*QDA-pyruvate which was added at the same concentration to every sample. The normalized ion counts of QDA- $^{13}\text{C}_3$ -pyruvate were then plotted against the known concentrations of 2.5, 5, and 7.5  $\mu\text{M}$  in buffer conditions and cell extract conditions to obtain linear regression equations. The ion suppression factor was then calculated from the ratio of the slopes of the two linear regressions.

The concentration of endogenous pyruvate was then calculated using the standard curve established by the internal standard QDA- $^{13}\text{C}_3$  pyruvate. Specifically, the normalized ion counts for QDA-pyruvate were averaged across three nine-minute FT-ICR-MS acquisitions, then over three replicate samples. Normalized ion counts of QDA-pyruvate from the blank (QDA added to buffer alone) were subtracted. This value was then used to calculate the  $\mu\text{M}$  concentration of endogenous pyruvate using the equation in Figure S2B in Supplementary information.

## 3 Results and Discussion

### 3.1 Probe design

The derivatizing agent **QDA** (Fig. 2) contains three structural domains: a carbonyl-selective aminoxy moiety, a quaternary ammonium ion for enhancing nanoelectrospray FT-ICR-MS sensitivity, and a hydrophobic aliphatic tail to enable organic phase extraction. We selected the aminoxy functional group over hydrazine and hydrazide functionality for its comparatively mild reaction conditions, stable reaction products (Kalia and Raines, 2008), and highly chemoselective oximation reaction with carbonyl substrates. We also synthesized a  $^{13}\text{C}^2\text{H}_3$ -labeled analog, \***QDA**, (Fig. 2) to highlight the QDA-derivatized metabolites among all charged species, as described below, and for improved quantification of endogenous carbonyl substrates.

### 3.2 Derivatization of carbonyl metabolites by aminoxy probe

Our probe was initially tested by derivatizing and partitioning four representative carbonyl standards, pyruvate,  $\alpha$ -ketoglutarate,  $\alpha$ -ketobutyrate, and glucose<sup>1</sup> from ammonium acetate buffer into *n*-butanol. As shown in Figure 3A, the \*QDA adducts of these standards were readily observed in the FT-ICR-MS spectra. To test the efficiency of the partitioning process, we repeatedly extracted the same standard adducts from buffer into *n*-butanol five times. This revealed that the majority of the adducts (*ca.* >98%) were recovered within the first two extractions (see Table S1 in Supplementary Information). Therefore, in subsequent cellular extract studies we performed three solvent partitions of the derivatized extracts to ensure high adduct recovery.

Figure 3B shows a representative FT-ICR-MS spectrum of QDA-derivatized A549 cell extracts, where the QDA adducts of endogenous pyruvate,  $\alpha$ -ketobutyrate,  $\alpha$ -ketoglutarate, and glucose were readily observed, along with multiple other QDA adducts. From the exact

<sup>1</sup>In the case of glucose, the aldehyde of the open-chain isomer is reactive with the probe.

masses, the molecular formulae of additional observed adducts were assigned. The partitioning of QDA adducts into *n*-butanol minimized the contribution of non-volatile salts such as NaCl and KCl to the final assay solution since their partitioning into *n*-butanol was reported to be low (0.02–0.1 wt % at 25 °C) (Li *et al.*, 1995). This was confirmed with our finding that the sodiated peaks of the adducts of spiked carbonyl standards extracted from A549 cell extract represented, on average, only 0.1% of the total ion count ( $H^+ + Na^+$ ) for a given adduct (data not shown). Such property is crucial to minimizing matrix salt interference for continuous infusion FT-ICR-MS analysis.

Although aminoxy functionality is known to be selective for reacting with carbonyl substrates (Rodriguez *et al.*, 1998), it can also react with epoxides at high concentrations, which we have tested on a model epoxide (glycidol) to be ca. 33% complete under the same reaction conditions. However, no known human epoxide metabolites (compiled from the KEGG database) were detected in the FT-ICR-MS spectra of A549 cell extracts when searched against their expected exact masses.

### 3.3 Stable isotope labeled aminoxy probe for global profiling of carbonyl metabolites

We prepared a  $^{13}CD_3$ -labeled analog of QDA by performing amine quaternization using  $^{13}CD_3I$  to obtain \*QDA (Fig. 2). Its value is two-fold: first, derivatization using \*QDA helps verify whether species observed in positive mode FT-ICR-MS are genuine carbonyl adducts of QDA as opposed to other *n*-butanol-soluble cellular metabolites (Johnson, 2007). Second, isotopic labeling enables quantitative analysis of carbonyl metabolites in cell extracts, as demonstrated below for pyruvate, the product of glycolysis and the entry metabolite of the Krebs cycle.

Figure 4 (top panel) illustrates how \*QDA made possible the global visualization of carbonyl metabolites in a crude human lung adenocarcinoma (A549) cell extract. QDA and \*QDA were added in equal amounts to an aqueous cell extract and then adducts were extracted as described above. This resulted in many pairs of adduct signals with comparable ion counts separated by 4.02188  $m/z$  ( $1 \times ^{13}C + 3 \times ^2H$ ). A given pair of adducts represented a carbonyl metabolite that has reacted with both derivatizing agents. Example QDA and \*QDA adduct pairs are delineated in Figure 4, where the full FT-ICR-MS spectrum (top inset) along with an expanded spectral region (bottom main panel) are shown. This spectrum was further processed as described in 2.5 to assign many likely carbonyl metabolites based on the derived molecular formulae of adducts and matching against a custom database that compiles the molecular formulae of many known carbonyl metabolites. These include  $\alpha$ -keto acids of the Krebs cycle (oxaloacetate and -ketoglutarate), carbohydrates (erythrose), lipid peroxidation products (eicosanal), oxidized amino acids (hydroxykynurenamine), nucleotide metabolites (deoxyribose), co-factors (pyridoxal-5-phosphate), and metabolites of glycolysis (pyruvate) and the pentose phosphate pathway (sedoheptulose). Table 1 is an abridged list of the QDA adducts assigned; the complete list is included in Table S2 in Supplementary information. Since structural isomers exist for many of these molecular formulae, the assignments shown here represent the most likely species based on known mammalian biochemistry. Further interrogation of these structural isomers by tandem MS and/or separation-based FT-ICR-MS methods is required to resolve their identity.

### 3.4 Estimation of extract matrix suppression and quantification of pyruvate

As described in Materials and Methods, an accurate quantification of carbonyl metabolites by the QDA method requires the consideration of several factors. Using pyruvate as an example, we verified the linear instrument response and estimated ion suppression effects of the extract matrix. In addition, an internal standard of  $^{13}C_3$ -pyruvate was used to correct for the effect of QDA reaction efficiency and solvent partitioning efficiency of the QDA

adducts on quantification. Pyruvate is a pivotal metabolite in mitochondrial Krebs cycle and anaplerotic pyruvate carboxylation (PC) for anabolic metabolism. PC has been recently shown to be activated in human lung cancer (Fan *et al.*, 2009).

The instrumental response for pyruvate and three other carbonyl metabolites is shown in Figure S1 (Supplementary Information) as scatter plots of ion counts versus concentrations. The linear regression parameters for the plots are listed in Table S3 (Supplementary Information). It is clear that the FT-ICR-MS instrument response was linear in the range from 0.025 to 25  $\mu\text{M}$  for all four metabolites. The ion suppression effect of the A549 cell extracts is illustrated in Figure 5, where the ion counts (normalized to the external  $^*\text{QDA}$ -pyruvate standard) of the internal  $[\text{U-}^{13}\text{C}]$ -pyruvate standard at three different concentrations were significantly higher for the buffer than for the cell extract matrices. The linear regression parameters of the normalized ion counts versus concentrations of the internal standard for both matrices are shown in Figure S2 (Supplementary information). The ratio of the two slopes revealed the ion suppression factor of 4.97 for cellular extracts.

With all these calibrations, we estimated the pyruvate concentration to be 0.4 nanomoles in *ca.* 625,000 cells or approximately 106 nmol/g cell wet weight, when cell numbers were calibrated against cell wet weight. This result is within the reported concentration range for pyruvate in serum (22–258  $\mu\text{M}$ ) (Psychogios *et al.*, 2011).

## 4 Conclusions

In summary, we have developed a new cationic aminoxy reagent for the selective derivatization of carbonyl metabolites in aqueous cell extracts. **QDA** is sufficiently amphiphilic that its oxime ether adducts can be extracted efficiently into *n*-butanol for rapid analysis by FT-ICR-MS. The **QDA** probe incorporates quaternary nitrogen to impart a permanent positive charge to the resulting adducts for optimal FT-ICR-MS detection. Furthermore, we have demonstrated a stable isotope labeling approach wherein  $^*\text{QDA}$  and **QDA** were used to generate mass spectral ion pairs separated by 4.02188 *m/z* for global profiling of carbonyl metabolites in crude extracts. When applied to human lung cancer A549 cell extracts, numerous carbonyl metabolites across multiple structural classes were assigned, including important metabolites of the central metabolic pathways. Thus, this approach enables both high sample and information throughput analysis of key components of the overall cellular oxidation state. Lastly, this approach can facilitate quantification of these often low-abundant and labile metabolites, as exemplified by the analysis of cellular pyruvate. As such, our chemoselective derivatization approach coupled with high resolution and sensitive FT-ICR-MS analysis can overcome the difficult challenge of mapping key carbonyl metabolites as well as cellular oxidation states which may be indicators for the onset of diseases.

## Supplementary Material

Refer to Web version on PubMed Central for supplementary material.

## Acknowledgments

We acknowledge financial support from NIH 1RO1CA118434-01A2 (TWMF), 3RO1CA118434-02S1 (TWMF), Kentucky Lung Cancer Research Program OGMB101380 (TWMF), and the University of Louisville Clinical & Translational Science Pilot Grant 20003. The FT-ICR-MS instrumentation at the Center for Regulatory and Environmental Analytical Metabolomics Mass Spectrometry Facility was funded by NSF/EPSCoR grant # EPS-0447479 (TWMF).

## References

- Barry SJ, Carr RM, Lane SJ, Leavens WJ, Manning CO, Monté S, Waterhouse I. Use of S-pentafluorophenyl tris(2,4,6-trimethoxyphenyl)phosphonium acetate bromide and (4-hydrazino-4-oxobutyl) [tris(2,4,6-trimethoxyphenyl)phosphonium bromide for the derivatization of alcohols, aldehydes and ketones for detection by liquid chromatography/electrospray mass spectrometry. *Rapid Communications in Mass Spectrometry*. 2003; 17:484–497. [PubMed: 12590398]
- Biswas S, Huang X, Badger WR, Nantz MH. Nucleophilic cationization reagents. *Tetrahedron Letters*. 2010; 51:1727–1729. [PubMed: 20204160]
- Eggink M, Wijtmans M, Kretschmer A, Kool J, Lingeman H, Esch IJPd, Niessen WMA, Irth H. Targeted LC–MS derivatization for aldehydes and carboxylic acids with a new derivatization agent 4-APEBA. *Anal Bioanal Chem*. 2010; 397:665–675. [PubMed: 20238107]
- Fan T, Lane A, Higashi R, Yan J. Stable isotope resolved metabolomics of lung cancer in a SCID mouse model. *Metabolomics*. 2011; 7:257–269. [PubMed: 21666826]
- Fan TW, Lane AN, Higashi RM, Farag MA, Gao H, Bousamra M, Miller DM. Altered regulation of metabolic pathways in human lung cancer discerned by (13)C stable isotope-resolved metabolomics (SIRM). *Mol Cancer*. 2009; 8:41. [PubMed: 19558692]
- Fang K, Pan X, Huang B, Liu J, Wang Y, Gao J. Simultaneous Derivatization of Hydroxyl and Ketone Groups for the Analysis of Steroid Hormones by–GC MS. *Chromatographia*. 2010; 72:949–956.
- Griffiths WJ, Hornshaw M, Woffendin G, Baker SF, Lockhart A, Heidelberger S, Gustafsson M, Sjövall J, Wang Y. Discovering Oxysterols in Plasma: A Window on the Metabolome. *Journal of Proteome Research*. 2008; 7:3602–3612. [PubMed: 18605750]
- Griffiths WJ, Koal T, Wang Y, Kohl M, Enot DP, Deigner H-P. Targeted Metabolomics for Biomarker Discovery. *Angew Chem Int Ed*. 2010; 49:5426–5446.
- Grochowski E, Jurczak J. A New Synthesis of *O*-Alkylhydroxylamines. *Synthesis*. 1976:682–684.
- Hong H, Wang Y. Derivatization with Girard Reagent T Combined with LC-MS/MS for the Sensitive Detection of 5-Formyl-2'-deoxyuridine in Cellular DNA. *Anal Chem*. 2007; 79:322–326. [PubMed: 17194156]
- Iglesias J, Gallardo JM, Medina I. Determination of carbonyl compounds in fish species samples with solid-phase microextraction with on-fibre derivatization. *Food Chemistry*. 2010; 123:771–778.
- Johnson DW. A modified Girard derivatizing reagent for universal profiling and trace analysis of aldehydes and ketones by electrospray ionization tandem mass spectrometry. *Rapid Communications in Mass Spectrometry*. 2007; 21:2926–2932. [PubMed: 17676710]
- Kalia J, Raines RT. Hydrolytic Stability of Hydrazones and Oximes. *Angew Chem Int Ed*. 2008; 47:7523–7526.
- Lane AN, Fan TWM, Higashi RM. Isotopomer-based metabolomic analysis by NMR and mass spectrometry. *Biophysical Tools for Biologists*. 2008; 84:541–588.
- Lane AN, Fan TWM, Xie Z, Moseley HNB, Higashi RM. Isotopomer analysis of lipid biosynthesis by high resolution mass spectrometry and NMR. *Analytica Chimica Acta*. 2009; 651:201–208. [PubMed: 19782812]
- Li Z, Tang Y, Liu Y, Li Y. Salting effect in partially miscible systems of n-butanol-water and butanone-water. *Fluid Phase Equilibria*. 1995; 103:143–153.
- Lorkiewicz PK, Higashii RM, Lane AN, Fan TW-M. High information throughput analysis of nucleotides and their isotopically enriched isotopologues by direct-infusion FTICR-MS. *Metabolomics*. 2011
- Maboudou P, Mathieu D, Bachelet H, Wiart JF, Lhermitte M. Detection of oxidative stress. Interest of GC-MS for malondialdehyde and formaldehyde monitoring. *Biomedical Chromatography*. 2002; 16:199–202. [PubMed: 11920945]
- Mark M, Ross DAK, Colton Richard J. Selective detection of aldehydes and ketones by derivatization/secondary ion mass spectrometry. *International Journal of Mass Spectrometry and Ion Processes*. 1985; 63:141–148.
- Negre-Salvayre A, Auge N, Ayala V, Basaga H, Boada J, Brenke R, Chapple S, Cohen G, Feher J, Grune T, Lengyel G, Mann GE, Pamplona R, Poli G, Portero-Otin M, Riahi Y, Salvayre R, Sasson



- S, Serrano J, Shamni O, Siems W, Siow RCM, Wiswedel I, Zarkovic K, Zarkovic N. Pathological aspects of lipid peroxidation. *Free Radical Research*. 2010; 44:1125–1171. [PubMed: 20836660]
- Noda Y, Berlett BS, Stadtman ER, Aponte A, Morgan M, Shen RF. Identification of enzymes and regulatory proteins in *Escheria coli* that are oxidized under nitrogen, carbon, or phosphate starvation. *PNAS*. 2007; 104:18456–18460. [PubMed: 18003895]
- Psychogios N, Hau DD, Peng J, Guo AC, Mandal R, Bouatra S, Sinelnikov I, Krishnamurthy R, Eisner R, Gautam B, Young N, Xia J, Knox C, Dong E, Huang P, Hollander Z, Pedersen TL, Smith SR, Bamforth F, Greiner R, McManus B, Newman JW, Goodfriend T, Wishart DS. The Human Serum Metabolome. *PLoS ONE*. 2011; 6
- Rodriguez EC, Marcaurelle LA, Bertozzi CR. Aminoxy-, Hydrazide-, and Thiosemicarbazide-Functionalized Saccharides: Versatile Reagents for Glycoconjugate Synthesis. *The Journal of organic chemistry*. 1998; 63:7134–7135. [PubMed: 11672350]
- Sugaya N, Sakurai K, Nakagawa T, Onda N, Onodera S, Morita M, Tezuka M. Development of a Headspace GC/MS Analysis for Carbonyl Compounds (Aldehydes and Ketones) in Household Products after Derivatization with *o*-(2,3,4,5,6-Pentafluorobenzyl)-hydroxylamine. *Analytical Sciences*. 2004; 20:865–870. [PubMed: 15171296]
- Wheeler OH. The Girard Reagents. *Journal of Chemical Education*. 1968; 45:435–437.
- Wikoff WR, Anfora AT, Liu J, Schultz PG, Lesley SA, Peters EC, Gary Siuzdaka. Metabolomics analysis reveals large effects of gut microflora on mammalian blood metabolites. *Proceedings of the National Academy of Sciences of the United States of America*. 2009; 106:3698–3703. [PubMed: 19234110]
- Zajdel A, Wilczok A, Slowinski J, Orchel J, Mazurek U. Aldehydic lipid peroxidation products in human brain astrocytomas. *J Neurooncol*. 2007; 84:167–173. [PubMed: 17487452]

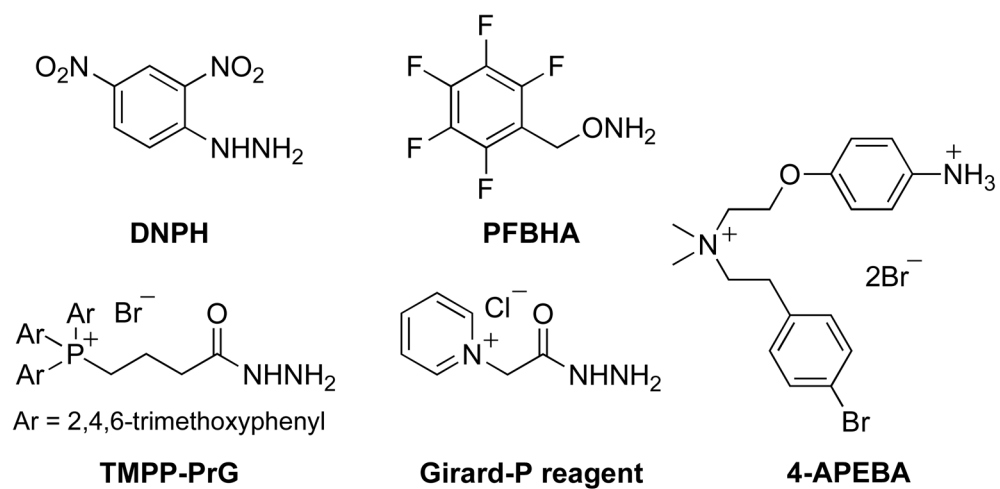


**Fig. 1.**  
Carbonyl derivatization agents for analysis by mass spectrometry

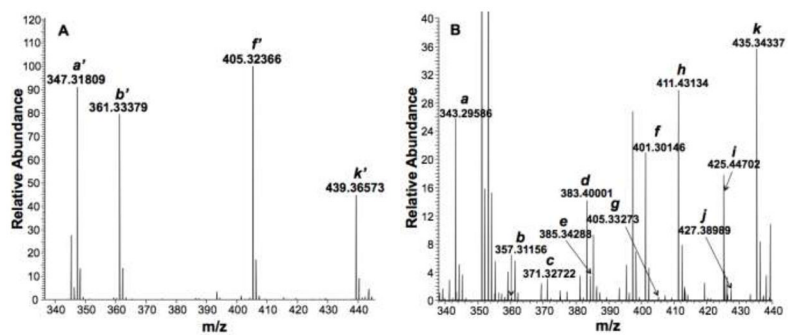


**Fig. 2.** Quaternary ammonium dodecyl aminoxy reagents, prepared as iodide salts

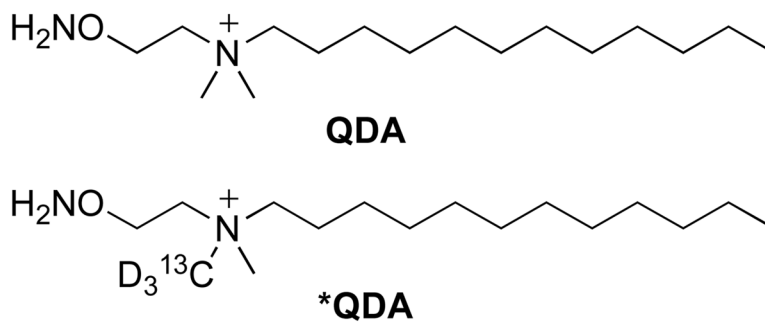


**Fig. 3. Derivatization of carbonyl standards and A549 cell extract**

*Panel A displays FT-ICR-MS spectrum of \*QDA adducts of four carbonyl standards after partitioning from ammonium acetate buffer into *n*-butanol: *a'* = pyruvate, *b'* =  $\alpha$ -ketobutyrate, *f* =  $\alpha$ -ketoglutarate, *k'* = glucose. The FT-ICR-MS spectrum of QDA-derivatized A549 cell extract is shown in panel B. *a* = pyruvate, *b* =  $\alpha$ -ketobutyrate, *c* = C<sub>7</sub>H<sub>14</sub>O, *d* = C<sub>8</sub>H<sub>16</sub>O, *e* = C<sub>6</sub>H<sub>10</sub>O<sub>3</sub>, *f* =  $\alpha$ -ketoglutarate, *g* = C<sub>5</sub>H<sub>10</sub>O<sub>5</sub>, *h* = C<sub>10</sub>H<sub>20</sub>O, *i* = C<sub>11</sub>H<sub>22</sub>O, *j* = C<sub>9</sub>H<sub>16</sub>O<sub>3</sub>, *k* = glucose.*

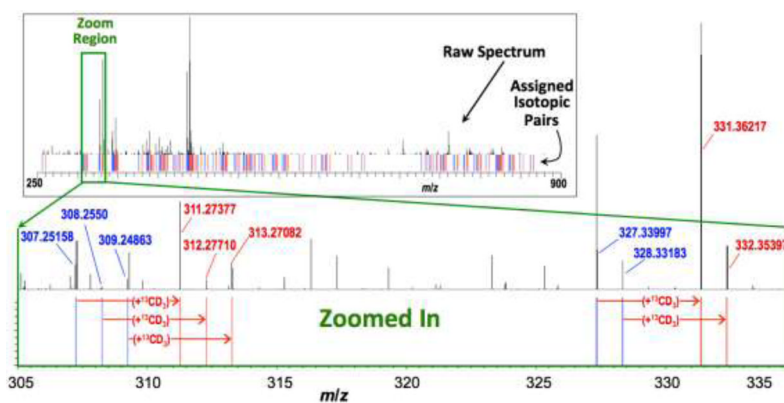


**Fig. 4. Companion unlabeled and labeled mass peaks reveal QDA adducts of carbonyl metabolites in A549 cancer cells**  
 The inset depicts the raw FT-ICR-MS spectrum of a QDA- + \*QDA-derivatized crude A549 cancer cell extract. Blue and red lines (below spectrum) respectively denote the  $m/z$  values of unlabeled and <sup>13</sup>CD<sub>3</sub>-labeled QDA derivatives, giving a “bar-code” profile of the derivative pairs. The mainpanel shows an expanded spectral region from the inset (as depicted by the green box) to more clearly illustrate the companion peaks.

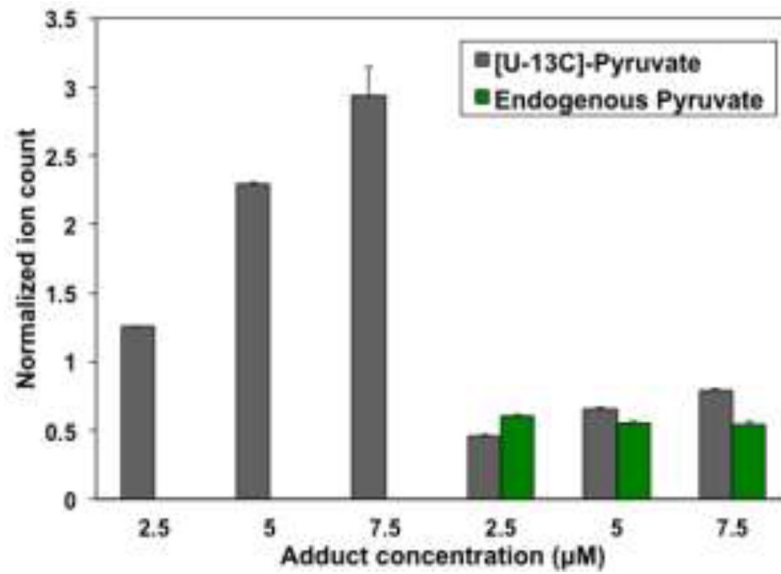


**Fig. 5.** Uniformly  $^{13}\text{C}$ -labeled pyruvate spiked at three concentrations into either buffer (left bars) or cell extract (right bars) and derivatized *in situ* with excess QDA. Ion counts were normalized against that of an external standard of  $2.5\ \mu\text{M}$  \*QDA-pyruvate.  $[\text{U-}^{13}\text{C}]\text{-Pyruvate} = \text{QDA-}^{13}\text{C}_3\text{-pyruvate}$ ; endogenous Pyruvate = QDA-pyruvate. Error bars represent one standard deviation over three injections of a single sample.

Table 1

Selected metabolites assigned based on Figure 4 Spectral Data

Mass isomer assignments	Molecular formula	Theoretical m/z for QDA adducts	Observed m/z	Mass error	Ion count
Pyruvate	C <sub>3</sub> H <sub>4</sub> O <sub>3</sub>	343.295519	343.295769	0.00025	905472.8
DHAP/ GAP <sup>a</sup>	C <sub>3</sub> H <sub>7</sub> O <sub>6</sub> P	425.277501	425.277999	0.000498	36810.4
Oxaloacetate	C <sub>4</sub> H <sub>4</sub> O <sub>5</sub>	387.285349	387.285619	0.00027	2621.8
D-Erythrose	C <sub>4</sub> H <sub>8</sub> O <sub>4</sub>	375.321734	375.322089	0.000355	22845.9
L-glutamate γ-semialdehyde	C <sub>5</sub> H <sub>9</sub> NO <sub>3</sub>	386.337718	386.338069	0.000351	33337.8
Deoxyribose	C <sub>5</sub> H <sub>10</sub> O <sub>4</sub>	389.337384	389.337689	0.000305	8659.2
α-Ketoglutarate	C <sub>5</sub> H <sub>6</sub> O <sub>5</sub>	401.300999	401.301469	0.00047	193346.3
5-Methylthio-D-ribose	C <sub>6</sub> H <sub>12</sub> O <sub>4</sub> S	435.325104	435.325029	-7.5E-05	2982.9
Hexose (ketose and aldose)	C <sub>6</sub> H <sub>12</sub> O <sub>6</sub>	435.342864	435.343289	0.000425	3235226.3
Hydroxykynurenamine	C <sub>9</sub> H <sub>12</sub> N <sub>2</sub> O <sub>2</sub>	435.369352	435.370609	0.001257	1106.1
Sedoheptulose	C <sub>7</sub> H <sub>14</sub> O <sub>7</sub>	465.353429	465.353969	0.00054	10502.8
oxo-dodecanoic acid	C <sub>12</sub> H <sub>22</sub> O <sub>3</sub>	469.436369	469.437049	0.00068	33371.2
S-(3-oxo-3-carboxy-n-propyl)cysteine	C <sub>7</sub> H <sub>11</sub> NO <sub>5</sub> S	476.315268	476.316249	0.000981	1017.3
N-Acetylhexosamine	C <sub>8</sub> H <sub>15</sub> NO <sub>6</sub>	476.369413	476.370119	0.000706	291404.4
5-isobutylthiortribose	C <sub>9</sub> H <sub>18</sub> O <sub>4</sub> S	477.372054	477.373469	0.001415	77115.6
Pyridoxal 5-phosphate	C <sub>8</sub> H <sub>10</sub> NO <sub>6</sub> P	502.30405	502.304809	0.000759	69620.1
Muramic acid	C <sub>9</sub> H <sub>17</sub> NO <sub>7</sub>	506.379978	506.380799	0.000821	3817.1
Octadecenal	C <sub>18</sub> H <sub>34</sub> O	521.540439	521.541639	0.0012	1657.1
Eicosanal	C <sub>20</sub> H <sub>40</sub> O	551.587389	551.588249	0.00086	26901.3

<sup>a</sup>DHAP: dihydroxyacetone phosphate; GAP: glyceraldehyde-3-phosphate.